Comparative toxicity of silver nanoparticles and silver ions to *Escherichia coli*

Yoojin Choi[1], Hyun-A Kim[2], Kyoung-Woong Kim[2], Byung-Tae Lee[2,*]

1. Department of Chemical and Biomolecular Engineering (BK21 Plus Program), Korea Advanced Institute of Science and Technology (KAIST), Daejeon 34141, Republic of Korea. E-mail: yjchoi216@kaist.ac.kr
2. School of Earth Sciences and Environmental Engineering, Gwangju Institute of Science and Technology (GIST), Gwangju 61005, Republic of Korea

ARTICLE INFO

ABSTRACT

With the increase in silver (Ag)-based products in our lives, it is essential to test the potential toxicity of silver nanoparticles (AgNPs) and silver ions (Ag ions) on living organisms under various conditions. Here, we investigated the toxicity of AgNPs with Ag ions to *Escherichia coli* K-12 strain under various conditions. We observed that both AgNPs and Ag ions display antibacterial activities, and that Ag ions had higher toxicity to *E. coli* K-12 strain than AgNPs under the same concentrations. To understand the toxicity of AgNPs at a cellular level, reactive oxygen species (ROS) enzymes were detected for use as antioxidant enzymatic biomarkers. We have also studied the toxicity of AgNPs and Ag ions under various coexistence conditions including: fixed total concentration, with a varied the ratio of AgNPs to Ag ions; fixed the AgNPs concentration and then increased the Ag ions concentration; fixed Ag ions concentration and then increasing the AgNPs concentration. Exposure to AgNPs and Ag ions clearly had synergistic toxicity; however, decreased toxicity (for a fixed AgNPs concentration of 5 mg/L, after increasing the Ag ions concentration) to *E. coli* K-12 strain. AgNPs and Ag ions in the presence of L-cysteine accelerated the bacterial cell growth rate, thereby reducing the bioavailability of Ag ions released from AgNPs under the single and coexistence conditions. Further works are needed to consider this potential for AgNPs and Ag ions toxicity across a range of environmental conditions.

Environmental Significance Statement: As silver nanoparticles (AgNPs)-based products are being broadly used in commercial industries, an ecotoxicological understanding of the AgNPs being released into the environment should be further considered. Here, we investigate the comparative toxicity of AgNPs and silver ions (Ag ions) to *Escherichia coli* K-12 strain, a representative ecotoxicological bioreporter. This study showed that toxicities of AgNPs and Ag ions to *E. coli* K-12 strain display different relationships when existing individually or when coexisting, and in the presence of L-cysteine materials. These findings suggest that the toxicology research of nanomaterials should consider conditions when NPs coexist with and without their bioavailable ions.

© 2017 The Research Center for Eco-Environmental Sciences, Chinese Academy of Sciences. Published by Elsevier B.V.

* *Corresponding author.* E-mail: btlee@gist.ac.kr (Byung-Tae Lee).

Introduction

Silver nanoparticles (AgNPs) are often used in antimicrobial and sterile applications such as cosmetics, clothing, and medicines based on their excellent antibacterial properties (Katz et al., 2015; Silver et al., 2006; Wei et al., 2015; Zhang et al., 2009). With the increasing interest and remarkable uses of AgNPs, it is becoming essential to consider the safety of such materials and the possible risks they pose to the environment (Handy et al., 2008; Nel et al., 2006). Undeniably, the toxicity of nanoparticles (NPs) to various organisms highlights a number of research issues in the field of environmental science (Kim et al., 2012; Lu et al., 2017; Wang et al., 2016a), with previous reports focusing on the toxicity of AgNPs to living organisms such as *Pseudomonas putida, Escherichia coli, Daphnia magna, Chlamydomonas reinhardtii, Cyprinus carpio, and Euglena gracilis* (Gaiser et al., 2012; Kim et al., 2016; Li et al., 2015; Matzke et al., 2014; Navarro et al., 2008b; Sondi and Salopek-Sondi, 2004; Wu et al., 2017). Based on this previous research, three major mechanisms of AgNPs toxicity to microorganisms have been suggested: (1) AgNPs can directly damage cell membranes, (2) AgNPs and silver ions (Ag ions) generate reactive oxygen species (ROS), and (3) AgNPs can release Ag ions (Marambio-Jones and Hoek, 2010).

AgNPs can also attach to the surface of living cells, where they interrupt the permeability and respiration of microorganisms (Dasgupta and Ramalingam, 2016; Steven and Fiedler, 2010). In addition, AgNPs might also act as a Trojan horse (*i.e.*, pass through cell barriers then release Ag ions inside) that damage living organisms (Lubick, 2008). Consequently, there are ongoing discussions about the roles of Ag ions that are released from AgNPs and their toxic effect on microorganisms. Some researchers have suggested that the toxicity of AgNPs is due to the NPs themselves, whereas others provide evidence that Ag ions released from AgNPs also play an important function (Park et al., 2009). When AgNPs release Ag ions, antibacterial activities are initiated by the Ag ions rather than AgNPs (Yin et al., 2011).

With regard to AgNPs- and Ag ions-based products, the major mechanism of toxicity to microorganisms is related to ROS (He et al., 2012; Hsin et al., 2008). ROS are short-lived reactive oxidants that include superoxide radicals (O_2^-), hydroxyl radicals (.OH), and hydrogen peroxide (H_2O_2) (Apel and Hirt, 2004). ROS can be generated in cells, and the oxidative stress results from a cellular defense system that includes antioxidant enzymes and antioxidants (Sondi and Salopek-Sondi, 2004). Large amounts of oxidative stress can subsequently lead to various problems and damage to proteins, lipids, and deoxyribonucleic acid (DNA) (Rahal et al., 2014). Antioxidant enzymes that act as ROS scavengers include superoxide dismutase (SOD), catalase (CAT), and glutathione peroxidase (GPX) (Pham-Huy et al., 2008). Note that glutathion (GSH) is typically present as a reduced form, where GSH is converted into its oxidized form glutathione disulfide (GSSG) *via* stimulation such as oxidative stress (Aquilano et al., 2014). In previous research, it was posited that the presence of AgNPs or Ag ions can lead to the generation of ROS, which then results in strong antibacterial activity (Maurer and Meyer, 2016; Wu and Zhou, 2013). However, there has been no precise quantitative estimate of the effect of AgNPs on *E. coli* K-12 strain was carried out. Therefore, detecting the amount of ROS scavengers is a well-known suitable method for monitoring the toxicity assessment; thus, understanding the ROS generated by AgNPs requires detecting the amount of ROS that was scavenged. Engineered NPs can be released into the environment by various routes; for example, during manufacturing, recycling, and disposal of relevant products (Navarro et al., 2008a; Nowack and Bucheli, 2007). In one analysis of the risk of releasing AgNPs into the ecosystem, it was predicted that 15% of the total Ag released into water in the European Union would be from Ag-based products (Blaser et al., 2008). Therefore, an ecotoxicological understanding of NPs in the environment should consider that AgNPs and Ag ions coexist (Nowack et al., 2012). Various other environmental conditions, affected by anions, cations, humic acids, and pH may also influence the characteristic properties of NPs (Gao et al., 2012; Levard et al., 2012). Therefore, researchers must consider and investigate the environmental fate and behavior of NPs under diverse environmental conditions (McGillicuddy et al., 2017; Ren et al., 2016). A previous report indicated that cysteine is a strong Ag ion ligand, one that proved helpful for surveying the role of Ag ions in the general toxicity of AgNPs (Navarro et al., 2008b). The thiol (– SH) group of cysteine can readily associate with Ag ions (Levard et al., 2012).

In this paper, we investigate and compare the toxicity of AgNPs and Ag ions to *E. coli* K-12 strain. *E. coli* has been well studied in-depth knowledge of its biochemistry and genetics, which makes it the most proficient prokaryote for the investigation of toxicological assays (Robbens et al., 2010). First, to determine the toxicity of AgNPs to *E. coli* K-12 strain, transmission electron microscopy (TEM) observations are used to bioaccumulation of AgNPs and detection of ROS was carried out. Second, we test the toxicity of AgNPs and Ag individually to *E. coli* K-12 strain. Third, we consider the toxicity of coexisting AgNPs and Ag ions to *E. coli* K-12 strain. Finally, the toxicity of AgNPs and Ag ions was combined with L-cysteine to create conditions that reduce the bioavailability of Ag ions released from AgNPs.

1. Materials and methods

1.1. Preparation and characterization of AgNPs

AgNP suspensions were purchased from Nanoleader, Korea and were dispersed ultrasonically (Powersonic 510, Hwasin Technology Company, Korea), and the physico-chemical properties of AgNPs were characterized. The core sizes and morphologies of the AgNPs were observed using TEM (JEOL 2100, Japan) at 200 kV and the hydrodynamic size and zeta potential were determined using dynamic light scattering (DLS; Zetasizer nano, Malvern, UK). The surface plasmon resonance was measured using a Ultraviolet–visible (UV-vis) spectrophotometer (UV-1601PC, Shimadzu, Japan). The mass concentration of AgNPs and Ag ions in the suspension was analyzed using ultracentrifugation (Amicon 3 kDa, Millipore, 2000 ×*g*, 30 min) and HNO_3 digestion, followed by inductively coupled plasma mass spectrometry (ICP-MS; Agilent 7500ce, USA) analysis; for

the Ag ion solution, an $AgNO_3$ (Sigma-Aldrich, USA, >99%) stock solution was prepared in distilled water.

1.2. Bacterial strain and cultivation

The microorganism used in this toxicity study was the bacterial strain *E. coli* K-12 (KCTC1116). The bacteria were grown in a Luria-Bertani (LB) medium (yeast extract 5%, trypton 5%, and NaCl 10%) at 37°C and 150 r/min, and the optical density (OD) of the suspension was determined at 600 nm using UV–vis.

1.3. TEM observation

TEM was used to observe the interactions between the AgNPs with *E. coli* K-12 strain and the bioaccumulation of AgNPs. The *E. coli* K-12 strain was exposed to 1, 5, or 10 mg/L of AgNPs (37°C with shaking at 150 r/min for 12 hr). For negative staining, the cells were washed with a phosphate buffered saline (PBS) solution, and then a 10 μL sample was dripped onto a TEM copper grid. To provide an intracellular TEM image, cells were collected after centrifugation at 1500 r/min for 5 min. The pellets were fixed in a mixture of 4% paraformaldehyde buffered with PBS (pH 7.4). Post-fixation was performed using 1% osmium tetroxide in the same buffer, with the cells being washed in PBS prior to fixation. Dehydration was accomplished by passage through a series of rising concentrations of ethanol (50%–100%), after which the samples were embedded in a Poly/Bed 812-Araldite medium (Polysciences Inc., USA) using propylene oxide. The samples were thin sectioned (less than 100 nm), and then double stained with uranyl acetate and lead citrate. Finally, the sections were mounted on TEM copper grids and examined at 120 kV (Tecnai G2, FEI, the Netherlands) at 120 kV.

1.4. Detection of ROS

To prepare samples, *E. coli* K-12 strain was exposed to 0 to 10 mg/L of AgNPs for 12 hr. To detect SOD enzymatic activity, the OxiSelect™ Superoxide Dismutase Activity Assay Kit was purchased from Cell Biolabs, USA. The absorbance of 96-plate samples was read at 490 nm on a microplate reader (μQuant, BIO-TEK, USA). To detect CAT enzymatic activity, the OxiSelect™ Catalase Assay Kit was purchased from Cell Biolabs, USA. Sample preparation was according to the manual provided. After sample treatment, we read the 96-plate absorbance at 520 nm using a microplate reader. Finally, we detected the total glutathione (GSSG/GSH) activity because glutathione protects the cells from free radical damage. To detect the total glutathione (GSSG/GSH) activity, the OxiSelect™ Glutathione Peroxide Cycle Assay Kit was purchased from Cell Biolabs, USA.

1.5. Individual toxicity of AgNPs and Ag ions

The test to determine the toxicity of AgNPs and Ag ions to *E. coli* K-12 strain, was divided into three conditions. In this experiment, *E. coli* K-12 strain not exposed to AgNPs or Ag ions was used as the control. To examine the inhibition of *E. coli* K-12 strain growth by AgNPs and Ag ions, bacterial cells were exposed to 1, 5, or 10 mg/L of AgNPs and Ag ions in a 100 mL

LB medium. Each flask was inoculated overnight from seed of the cultured *E. coli* K-12 strain, and then incubated for 12 hr at 37°C while shaking at 150 r/min.

1.6. Toxicity of coexisting AgNPs and Ag ions

The experiments used to determine the toxicity of coexisting AgNPs and Ag ions to *E. coli* K-12 strain, were divided into three conditions. First, we fixed the total concentration at 5 mg/L, but varied the ratio of AgNPs to Ag ions (1 mg/L AgNPs + 4 mg/L Ag ions, 2.5 mg/L AgNPs + 2.5 mg/L Ag ions, and 4 mg/L AgNPs + 1 mg/L Ag ions). Second, we fixed the AgNPs concentration of 5 mg/L and then increased the Ag ions concentration (5 mg/L + 1 mg/L Ag ions, 5 mg/L AgNPs + 2 mg/L Ag ions, 5 mg/L AgNPs + 3 mg/L Ag ions, and 5 mg/L AgNPs + 4 mg/L Ag ions). Third, we fixed the Ag ions concentration of 5 mg/L and then increased the AgNPs concentration (5 mg/L Ag ions + 1 mg/L AgNPs, 5 mg/L Ag ions + 2 mg/L AgNPs, 5 mg/L Ag ions + 3 mg/L AgNPs, and 5 mg/L Ag ions + 4 mg/L AgNPs). Each flask was inoculated overnight with seed from the cultured strain and incubated for 12 hr at 37°C while shaking at 150 r/min.

1.7. Toxicity of AgNPs and Ag ions under L-cysteine

We also investigated the toxicity of AgNPs and Ag ions to *E. coli* K-12 strain under various conditions of 10 mmol/L L-cysteine (≥98%, Sigma-Aldrich, USA). To determine the inhibition of *E. coli* K-12 strain growth, the cells were exposed to different conditions of 10 mmol/L L-cysteine in 100 mL of LB medium. Each flask was inoculated overnight with a seed of the cultured *E. coli* K-12 strain and incubated for 12 hr at 37°C while shaking at 150 r/min. The experiments used to determine the toxicity of coexisting AgNPs and Ag ions with L-cysteine to *E. coli* K-12 strain, were divided into three conditions. First, we fixed total Ag concentration of 5 mg/L, but varied the ratio of AgNPs to Ag ions with 10 mmol/L L-cysteine (1 mg/L AgNPs + 4 mg/L Ag ions, 2.5 mg/L AgNPs + 2.5 mg/L Ag ions, and 4 mg/L AgNPs + 1 mg/L Ag ions). Second, we fixed the AgNPs concentration of 5 mg/L and then increased the Ag ions concentration with 10 mmol/L L-cysteine (5 mg/L AgNPs + 1 mg/L Ag ions, 5 mg/L AgNPs + 2 mg/L Ag ions, 5 mg/L AgNPs + 3 mg/L Ag ions, and 5 mg/L AgNPs + 4 mg/L Ag ions). Third, we fixed the Ag ions concentration of 5 mg/L and then increased the AgNPs concentration with 10 mmol/L L-cysteine (5 mg/L Ag ions + 1 mg/L AgNPs, 5 mg/L Ag ions + 2 mg/L AgNPs, 5 mg/L Ag ions + 3 mg/L AgNPs, and 5 mg/L Ag ions + 4 mg/L AgNPs). Each flask was inoculated overnight with seed from the cultured strain and incubated for 12 hr at 37°C with shaking at 150 r/min.

1.8. Calculation of the cell number and growth rates

The number of cells was measured using the 12 hr OD_{600} obtained using a UV–vis spectrophotometer. After each observation, we calculated that the number of cells based on $OD_{600} = 0.1$ is equal to 10^8 cells/mL. Moreover, the growth rate (r, hr^{-1}) of the cells was calculated and then compared to the trend in toxicity using Eq. (1):
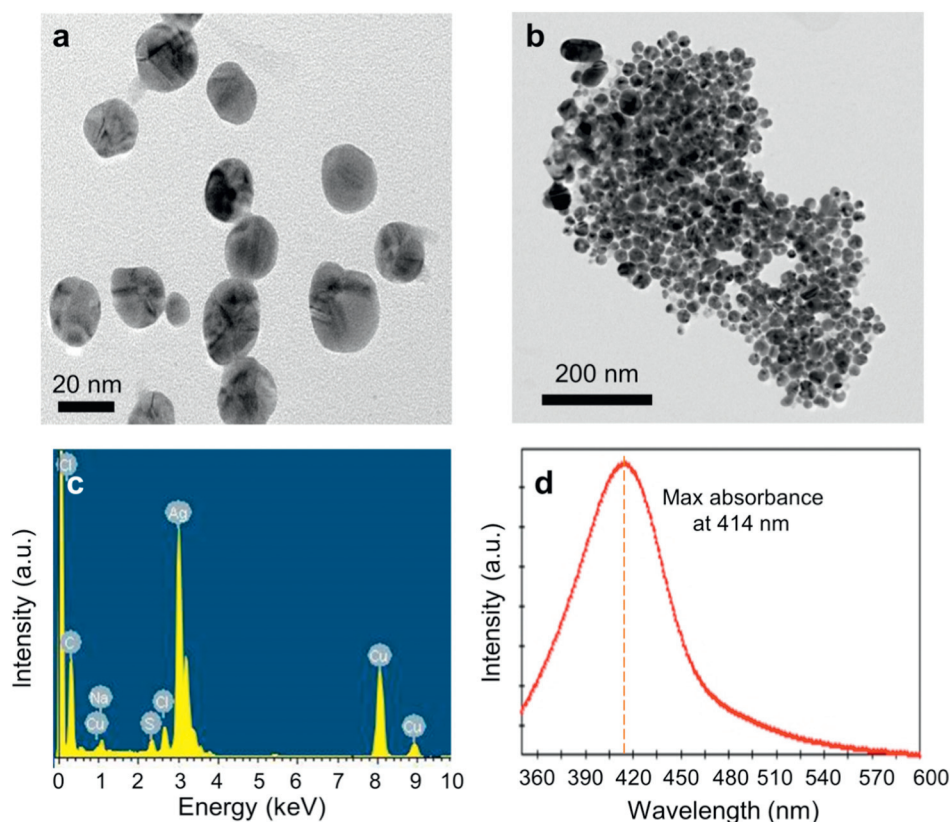
$$r = dN/dt \qquad (1)$$

Fig. 1 – Characterization of engineered AgNPs. TEM images of (a) engineered AgNPs in distilled water and (b) engineered AgNPs in LB medium. (c) EDS analysis of AgNPs and (d) UV spectrum of AgNPs. AgNPs: silver nanoparticles; TEM: transmission electron microscopy; LB: Luria-Bertani; EDS: energy-dispersive X-ray spectroscopy; UV: ultraviolet–visible.

where, N ($\times 10^8$ cells/mL) is the number of cells; t (hr) is the time during experiments.

We calculated the growth rate and compared the initial and final growth rates during 12 hr, under the conditions in which AgNPs and Ag ions coexisted, in the presence of L-cysteine. The initial time represents an incubation time of 0 to 4 hr of incubation time, and the final time represents an incubation time of 8 to 12 hr.

1.9. Statistical analysis

All the experiments were performed at least in triplicate. The data collected were investigated using the statistical program SigmaPlot 10.0 (SPSS Inc., USA). The statistical significances of the differences between the control and test groups were analyzed using a one-way analysis of variance (ANOVA) by Duncan's comparison. A 95% significance level ($p < 0.05$) was considered to be significant.

2. Results

2.1. Characterization of AgNPs

To confirm the characteristics of the engineered AgNPs used in this study, we investigated their size with TEM, hydrodynamic size (0.1 mmol/L $NaNO_3$) by DLS, zeta potential (at pH 7.2), UV spectrum, and morphology (Fig. 1 and Table 1). We observed the morphology and aggregation of AgNPs in distilled water and in the Luria-Bertani (LB) medium (Fig. 1a, b). AgNPs are seen to have a round shape and are well-dispersed in DI water, whereas the AgNPs more frequently aggregated and form particles in the LB medium. The energy-dispersive X-ray spectroscopy (EDS) analysis indicated that the main element was Ag after the AgNPs were exposed to the LB medium (Fig. 1c), and that the AgNPs have a maximum peak at 414 nm in the UV spectrum (Fig. 1d). From

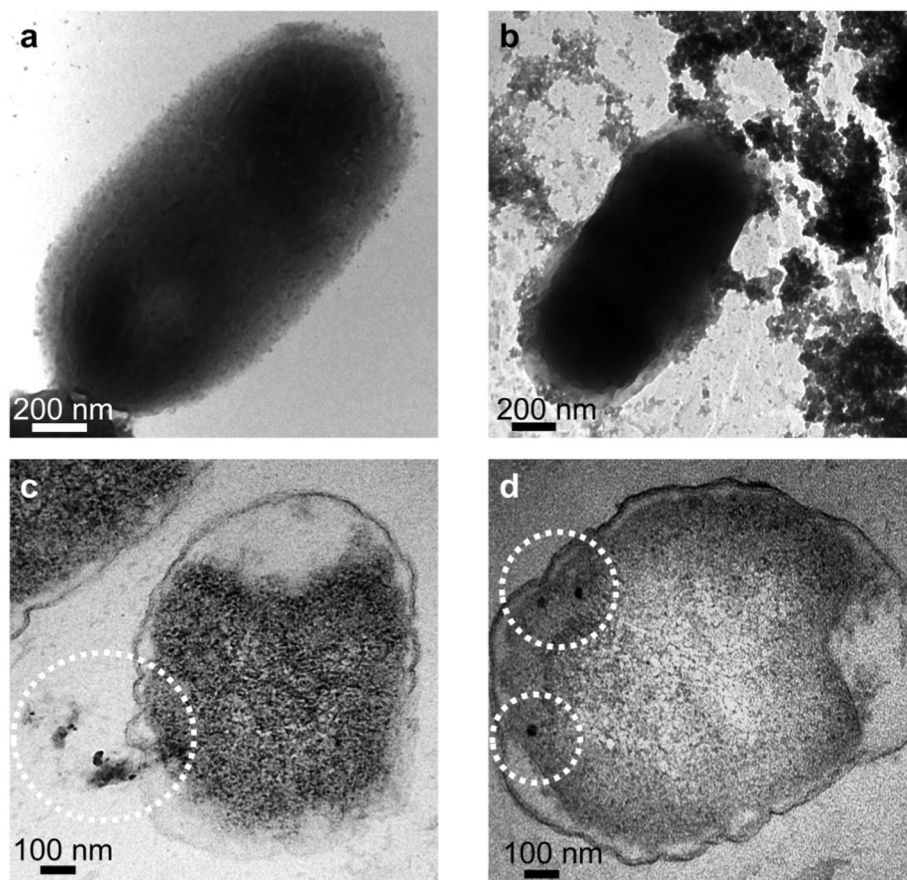| Table 1 – Characteristics of engineered AgNPs.				
Average size by TEM	Hydrodynamic size by DLS (0.1 mmol/L $NaNO_3$)	Zeta potential (at pH 7.2)	UV 1st peak position	Dissolved Ag ions in stock solution
23.6 nm	57.8 nm	−28.3 mV	414 nm	7.1%
DLS: dynamic light scattering; UV: ultraviolet–visible.				

Fig. 2 – TEM image of *E. coli* K-12 strain exposed to (a) 1 mg/L AgNPs, (b) 10 mg/L AgNPs, and cross sectioned *E. coli* K-12 strain exposed to (c) 1 mg/L AgNPs, and (d) 10 mg/L AgNPs for 12 hr.

the TEM image, the average diameter of the AgNPs is 23.6 nm, and the hydrodynamic size was 57.8 nm, as indicated by DLS (Table 1). The zeta potential was −28.3 mV at pH 7.2, because the AgNPs have a negatively charged surface. The mass fraction of the dissolved Ag ions in the stock solution was 7.1%.

2.2. TEM observations of *E. coli* K-12 strain after AgNPs treatment

We examined the TEM image of *E. coli* morphology after exposure to the cell to AgNPs for 12 hr. When the bacterial
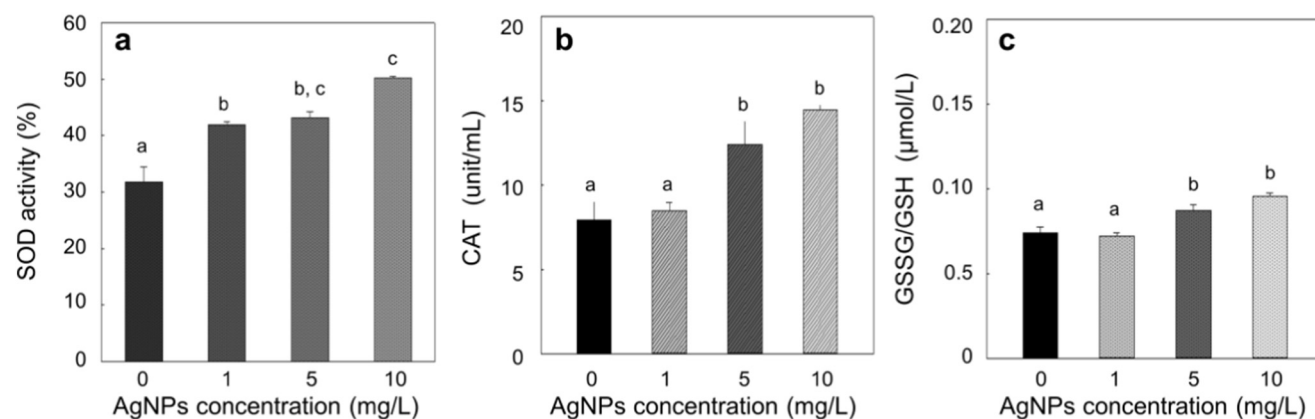

Fig. 3 – Detection of (a) SOD, (b) CAT, and (c) GSSG/GSH using enzyme activity for *E. coli* K-12 strain at various AgNP concentrations for 12 hr. Experiments were conducted in triplicates. Error bars indicate Standard Deviation (S.D.). Values of each enzyme activities followed by different letters (a, b, and c) above the bars indicate that the data points are significantly different at $p < 0.05$. SOD: superoxide dismutase; CAT: catalase; AgNP: silver nanoparticle; GSSG: glutathione disulfide; GSH: glutathione.

cells were exposed to 1 mg/L AgNPs, the AgNPs surrounded the membrane (Fig. 2a); after exposure to 10 mg/L AgNPs (Fig. 2b), the AgNPs enveloped the cell. From these results, it is clear that the AgNPs significantly attached to the cell surface and interacted with the membrane.

In the intracellular images, when *E. coli* K-12 strain was exposed to 1 mg/L AgNPs for 12 hr, the cell membrane displayed clear damage (Fig. 2c). Interestingly, the AgNPs were bioaccumulated and aggregated within the cell after

exposure to 10 mg/L AgNPs (Fig. 2d). The circle in the figure shows that the AgNPs penetrated through the cell membrane and that there was an intracellular uptake of AgNPs within the cells.

2.3. Generation of ROS by AgNPs

To determine the cellular ROS level after exposure to AgNPs for 12 hr, we detected the generation of ROS in the forms of SOD,
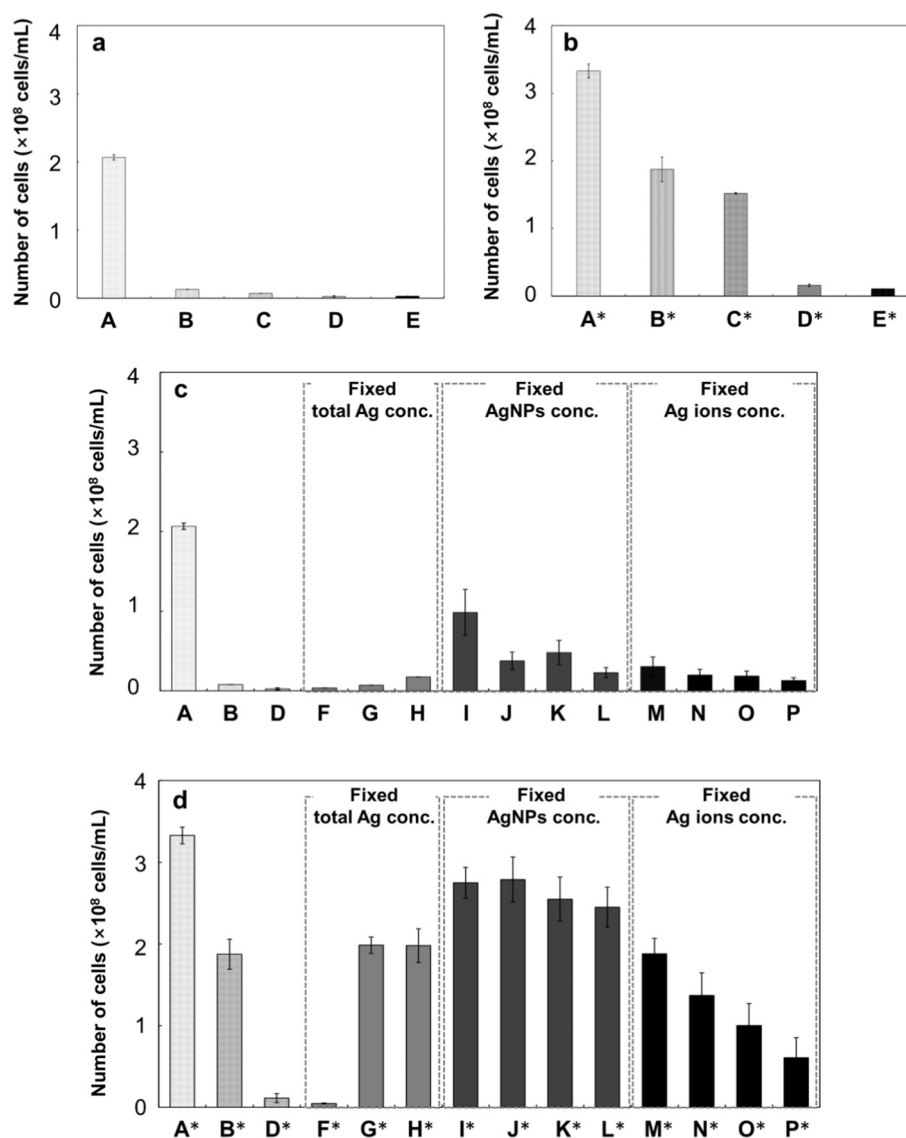

Fig. 4 – Growth inhibition of *E. coli* K-12 strain by AgNPs and Ag ions under various conditions. Experiments were conducted in triplicates. Error bars indicate S.D. (a) Growth inhibition of *E. coli* K-12 strain by AgNPs and Ag ions at 6 hr, (b) growth inhibition of *E. coli* K-12 strain by AgNPs and Ag ions at 12 hr, (c) various exposure conditions at 6 hr, and (d) various exposure conditions at 12 hr. Note: Native *E. coli* K-12 strain as control at 6 hr for A and 12 hr for A*; 5 mg/L AgNPs at 6 hr for B and at 12 hr for B*; 10 mg/L AgNPs at 6 hr for C and at 12 hr for C*; 5 mg/L Ag ions at 6 hr for D and at 12 hr for D*; 10 mg/L Ag ions at 6 hr for E and at 12 hr for E*; 1 mg/L AgNPs + 1 mg/L Ag ions at 6 hr for F and at 12 hr for F*; 2.5 mg/L AgNPs + 2.5 mg/L Ag ions at 6 hr for G and at 12 hr for G*; 4 mg/L AgNPs + 1 mg/L Ag ions at 6 hr for H and at 12 hr for H*; 5 mg/L AgNPs + 1 mg/L Ag ions at 6 hr for I and at 12 hr for I*; 5 mg/L AgNPs + 2 mg/L Ag ions at 6 hr for J and at 12 hr for J*; 5 mg/L AgNPs + 3 mg/L Ag ions at 6 hr for K and at 12 hr for K*; 5 mg/L AgNPs + 4 mg/L Ag ions at 6 hr for L and at 12 hr for L*; 5 mg/L Ag ions + 1 mg/L AgNPs at 6 hr for M and at 12 hr for M*; 5 mg/L Ag ions + 2 mg/L AgNPs at 6 hr for N and at 12 hr for N*; 5 mg/L Ag ions + 3 mg/L AgNPs at 6 hr for O and at 12 hr for O*; 5 mg/L Ag ions + 4 mg/L AgNPs at 6 hr for P and at 12 hr for P*. S.D.: Standard Deviation.

Table 2 – Calculation of initial time (0 to 4 hr) growth rate and final time (8 to 12 hr) growth rate of *E. coli* K-12 strain with AgNPs and Ag ions under different exposure conditions.

Conditions	AgNPs (mg/L)	Ag ions (mg/L)	Initial growth rate (hr^{-1})	Final growth rate (hr^{-1})	Initial growth rate with 10 mmol/L cysteine (hr^{-1})	Final growth rate with 10 mmol/L cysteine (hr^{-1})
Single exist conditions						
E. coli K-12 strain	0	0	0.392	0.314	0.266	0.020
AgNPs	5	0	0.021	0.292	0.245	0.060
	10	0	0.021	0.342	0.210	0.029
Ag ions	0	5	0.011	0.023	0.162	0.023
	0	10	0.001	0.001	0.169	0.143
Coexist conditions						
Fixed total Ag concentration at 5 mg/L	1	4	0.001	0.003	0.260	0.039
	2.5	2.5	0.004	0.256	0.251	0.001
	4	1	0.001	0.133	0.243	0.060
Fixed AgNPs concentration of 5 mg/L	5	1	0.112	0.390	0.274	0.142
	5	2	0.068	0.513	0.277	0.189
	5	3	0.020	0.446	0.281	0.168
	5	4	0.014	0.490	0.280	0.113
Fixed Ag ions concentration of 5 mg/L	1	5	0.015	0.256	0.368	0.006
	2	5	0.008	0.132	0.392	0.005
	3	5	0.009	0.099	0.390	0.006
	4	5	0.009	0.036	0.405	0.065

CAT, and GSSG/GSH enzyme activity (Fig. 3). AgNPs at 1 and 5 mg/L AgNPs induced the same SOD activity groups, with both having a similar SOD activity (Fig. 3a), *i.e.*, the AgNPs induced oxidative stress in the *E. coli* K-12 strain and the antioxidant enzyme SOD was activated. The CAT enzyme activity dramatically increased with increasing AgNPs concentration (Fig. 3b), whereas GSSG/GSH enzyme activity showed only slight differences at different AgNP concentrations (Fig. 3c). Based on the results, these three different ROS enzymes showed different activities after *E. coli* K-12 strain was treated with the same concentrations of AgNPs. Therefore, AgNPs induced oxidative stress in *E. coli* K-12 strain and these three antioxidant enzymes were activated.

2.4. Toxicity of AgNPs or Ag ions when tested individually

The number of cells and the bacterial growth rates were measured to investigate the toxicity of AgNPs or Ag ions tested individually on *E. coli* K-12 strain (Fig. 4a and Table 2). The number of cells indicated the toxicity end point after treatment with AgNPs or Ag ions, each for 6 or 12 hr. When the cells were exposed to 5 or 10 mg/L of AgNPs and Ag ions, the number of cells decreased as the concentration was increased (Appendix A Fig. S1). In addition, Ag ions were seen to be much more toxic to *E. coli* K-12 strain than the AgNPs. Cell growth inhibition was observed for *E. coli* after each treatment with AgNPs or Ag ions each for 12 hr. After treatment, only a few cells had grown during the initial growth period (Table 2 and Appendix A Fig. S2a); however, by the end of the growth period, the cellular growth rate had increased more than 10 times (Table 2 and Appendix A Fig. S2b). Therefore, AgNPs and Ag ions are deemed to be toxic to *E. coli* K-12 strain, relative to their increasing concentration and their ability to inhibit the growth of *E. coli* K-12 strain.

2.5. Toxicity of AgNPs and Ag ions in coexist conditions

We investigated the difference in toxicity of AgNPs and Ag ions to *E. coli* K-12 strain in a solution under different conditions of coexistence after 12 hr (Fig. 4b, c). First, the toxicity on *E. coli* K-12 strain was investigated at different ratios of AgNPs to Ag ions, at a fixed total Ag concentration of 5 mg/L (Figs. 4b,c and Appendix A Fig. S3). After 12 hr, the number of cells showed the same trend for 4 mg/L AgNPs after adding 1 mg/L Ag ions, as for 2.5 mg/L AgNPs after adding 2.5 mg/L Ag ions. However, a further increase in the proportion of Ag ions in the mixture increased the toxicity. We also calculated the initial and final cell growth at a fixed total Ag concentration of 5 mg/L (Table 2 and Appendix A Fig. S4). The initial cell growth represents the increase in the proportion of Ag ions in the mixture, and over time the growth rate decreased; under the same conditions, the final growth rate was significantly less.

We then examined the toxicity effect on *E. coli* K-12 strain at a fixed AgNPs concentration of 5 mg/L, after increasing the Ag ions concentration (Figs. 4b,c and Appendix A Fig. S5). The numbers of cells grown displayed similar trend as the toxicity, even after increasing the Ag ions concentration. Interestingly, the toxicity was less than that for 5 mg/L AgNPs only, and the final growth rate was dramatically increased (Table 2 and Appendix A Fig. S6).

Finally, we tested the toxicity effect on *E. coli* K-12 strain at fixed Ag ions concentration of 5 mg/L, after increasing the AgNPs concentration (Figs. 4b,c and Appendix A Fig. S7). Under this coexistence, the number of cells was inhibited because of the Ag ions toxicity. The initial growth rate was slightly decreased with increases in the AgNPs concentration (Table 2 and Appendix A Fig. S8a), with the final growth rate being significantly decreased under these same conditions (Appendix A Fig. S8b).

2.6. Toxicity of AgNPs and Ag ions with L-cysteine

In this series of tests, we first analyzed the effect of only AgNPs using L-cysteine, and investigated the toxicity of AgNPs itself without the effect of released Ag ions. We then tested the toxicity

effect on *E. coli* of both AgNPs and Ag ions with L-cysteine, under various exposure conditions (Figs. 5 and Appendix A Figs. S8–9). The number of *E. coli* K-12 strain cells present after being treated with AgNPs and Ag ions with L-cysteine decreased, though the initial and final cell growth increased (Figs. 5a and Appendix A
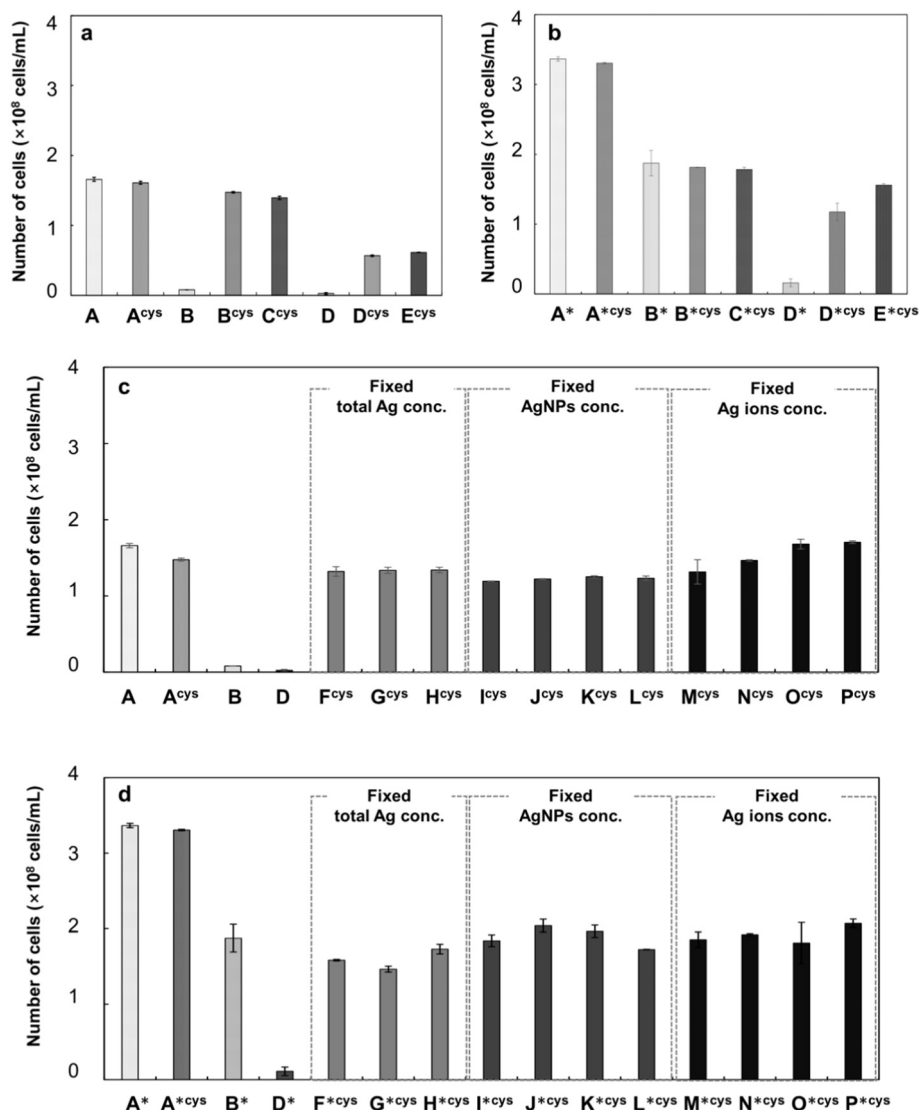

Fig. 5 – Growth inhibition of *E. coli* K-12 strain by AgNPs and Ag ions with 10 mmol/L L-cysteine after treatment under various conditions. Experiments were conducted in triplicates. Error bars indicate S.D. (a) Growth inhibition of *E. coli* K-12 strain by AgNPs and Ag ions with L-cysteine at 6 hr, (b) growth inhibition of *E. coli* K-12 strain by AgNPs and Ag ions with L-cysteine at 12 hr, (c) various exposure conditions with L-cysteine at 6 hr, and (d) various exposure conditions with L-cysteine at 12 hr. Note: A, B, D and A*, B*, D* are the same as Fig. 4; native *E. coli* K-12 strain with 10 mmol/L L-cysteine at 6 hr for A^{cys} and at 12 hr for A^{*cys}; 5 mg/L AgNPs with 10 mmol/L L-cysteine at 6 hr for B^{cys} and at 12 hr for B^{*cys}; 10 mg/L AgNPs with 10 mmol/L L-cysteine at 6 hr for C^{cys} and at 12 hr for C^{*cys}; 5 mg/L Ag ions with 10 mmol/L L-cysteine at 6 hr for D^{cys} and at 12 hr for D^{*cys}; 10 mg/L Ag ions with 10 mmol/L L-cysteine at 6 hr for E^{cys} and at 12 hr for E^{*cys};: 1 mg/L AgNPs + 1 mg/L Ag ions with 10 mmol/L L-cysteine at 6 hr for F^{cys} and at 12 hr for F^{*cys}; 2.5 mg/L AgNPs + 2.5 mg/L Ag ions with 10 mmol/L L-cysteine at 6 hr for G^{cys} and at 12 hr for G^{*cys}; 4 mg/L AgNPs + 1 mg/L Ag ions with 10 mmol/L L-cysteine at 6 hr for H^{cys} and at 12 hr for H^{*cys};: 5 mg/L AgNPs + 1 mg/L Ag ions with 10 mmol/L L-cysteine at 6 hr for I^{cys} and at 12 hr for I^{*cys}; 5 mg/L AgNPs + 2 mg/L Ag ions with 10 mmol/L L-cysteine at 6 hr for J^{cys} and at 12 hr for J^{*cys}; 5 mg/L AgNPs + 3 mg/L Ag ions with 10 mmol/L L-cysteine at 6 hr for K^{cys} and at 12 hr for K^{*cys}; 5 mg/L AgNPs + 4 mg/L Ag ions with 10 mmol/L L-cysteine at 6 hr for L^{cys} and at 12 hr for L^{*cys}; 5 mg/L Ag ions + 1 mg/L AgNPs with 10 mmol/L L-cysteine at 6 hr for M^{cys} and at 12 hr for M^{*cys}; 5 mg/L Ag ions + 2 mg/L AgNPs with 10 mmol/L L-cysteine at 6 hr for N^{cys} and at 12 hr for N^{*cys}; 5 mg/L Ag ions + 3 mg/L AgNPs with 10 mmol/L L-cysteine at 6 hr for O^{cys} and at 12 hr for O^{*cys}; 5 mg/L Ag ions + 4 mg/L AgNPs with 10 mmol/L L-cysteine at 6 hr for P^{cys} and at 12 hr for P^{*cys}.

Figs. S9–10). When 10 mmol/L of L-cysteine was added, the number of cells was extremely increased during 12 hr, even for a 10 mg/L concentration of Ag ions (Figs. 5a and Appendix A Fig. S11). Furthermore, the initial growth rate of E. coli K-12 strain significantly increased when 10 mmol/L L-cysteine was added to AgNPs or Ag ions in individually (Table 2 and Appendix A Fig. S12). Overall, the initial growth rate was seen to dramatically increase, and just only slightly different from the final growth rate with L-cysteine.

We then confirmed the toxicity on E. coli by AgNPs and Ag ions under different conditions of coexistence with L-cysteine. First, with the Ag total concentration fixed at 5 mg/L, and with 10 mmol/L L-cysteine added, the number of cells was low when the proportion of Ag ions was high (Figs. 5b and Appendix A Fig. S13). There was no difference in the trend in the growth rate of E. coli K-12 strain in this case, from that when increasing the proportion of Ag ions in the mixture (Table 2 and Appendix A Fig. S14).

Next, we fixed the AgNPs concentration of 5 mg/L and increased both the Ag ions and 10 mmol/L L-cysteine (Figs. 5c and Appendix A Fig. S15). The results indicate the same trend in toxicity for 5 mg/L AgNPs alone. The decrease in toxicity for 5 mg/L AgNPs + 4 mg/L Ag ions with L-cysteine was comparable to the results without L-cysteine. Overall, the initial growth rate of E. coli K-12 strain was greater, even though the concentration of Ag ions was increased under these conditions (Table 2 and Appendix A Fig. S16).

We then fixed the concentration of Ag ions of 5 mg/L, and increased the AgNPs concentration while adding 10 mmol/L L-cysteine (Fig. 5d). In this case, the number of cells increased, even though the concentration of Ag ions increased (Appendix A Fig. S17). Ultimately, the effect of L-cysteine was to increase the initial growth rate of E. coli K-12 strain simultaneously treated with AgNPs and Ag ions, as compared to the growth rate observed under Ag ions with no L-cysteine (Table 2 and Appendix A Fig. S18).

3. Discussion

We investigated and verified here the toxicity mechanism of AgNPs on E. coli K-12 strain, as well as the bacterial interaction with AgNPs (Fig. 2) and the generation of ROS within the cells (Fig. 3). The negatively charged AgNPs were seen to easily interact with the positively charged cell surfaces (Frohlich, 2012; Weiss and Zeigel, 1971). AgNPs were found to attach to the cell surface and displayed intracellular accumulation after treatment with 10 mg/L AgNPs (Fig. 2d). Based on a molecular-dynamics simulation, a possible mechanism for this behavior was that a representative lipid bilayer is permeable to buckyball-sized nanomolecules (Steven and Fiedler, 2010). It was also shown that the bioaccumulation of some metals can form uncharged lipophilic complexes with organic ligands that can pass through membranes by passive diffusion (Ratte, 1999). Therefore, it is posited here that AgNPs are subject to intracellular accumulation, making it possible for them to affect the cellular metabolism.

Furthermore, to understand the toxicity of AgNPs to E. coli K-12 strain at the intracellular level, ROS substances were generated (e.g., SOD, CAT, and GSSG/GSH) as antioxidant enzymes were detected after cells were exposed to various concentrations of AgNPs. The results of this study suggest that the toxicity mechanism to E. coli K-12 strain of AgNPs is related to oxidative damage. The activities of these three enzymes increased with increases in the AgNPs concentration, with the scavenging enzyme activities providing information about the stimulation of oxidative stress in E. coli K-12 strain. In this research, the CAT enzyme was the most sensitive for detecting E. coli K-12 strain exposed AgNPs (Fig. 3b); therefore, the CAT enzyme is seen to be a useful antioxidant enzyme that defends against oxidative stress, and a major biomarker for highlighting E. coli K-12 strain exposure to AgNPs. It could thus be confirmed that the toxicity mechanism of AgNPs in E. coli K-12 strain is related to oxidative damage from chemical species such as O_2^- and H_2O_2. Previous researchers reported that SOD, CAT, and GSSG/GSH correspond to increases in apoptotic cell death (Buffet et al., 2013; Xu et al., 2012). Overall, the increasing and decreasing activity of antioxidant enzymes was reported to depend on the microbial species, NP characteristics such as size and crystallite, and exposure conditions (Lu et al., 2017).

In previous research, the toxicity of NPs is fully dependent on the water chemistry, and several exposure conditions have to be considered in order to identify the toxicity of AgNPs to microorganisms (Peng et al., 2017; Wang et al., 2016b; Zhang et al., 2015). Here, a comparative study was carried out to investigate the toxicity of AgNPs and Ag ions to E. coli K-12 strain under different conditions. AgNPs and Ag ions display a significant antibacterial activity toward E. coli K-12 strain when tested independently (Fig. 4a). After E. coli K-12 strain was exposed, it became clear that Ag ions showed greater toxicity, and inhibited bacterial cell growth more, than AgNPs. The calculation of growth rates revealed that Ag ions induced a slow initial growth rate (Table 2), i.e., therefore, AgNPs and Ag ions inhibited the initial growth, and that the bacterial cells needed time, at first, for detoxification.

Ag ions were also the dominant toxicity factor for E. coli K-12 strain under the condition of AgNPs and Ag ions coexisting (Fig. 4b–d). Based on these results, the initial inhibition of E. coli K-12 strain growth by Ag ions was observed, though the growth became much more active later (Table 2). Therefore, Ag ions can inhibit the cell growth rate, when the concentration of Ag ions is higher under the condition of coexisting AgNPs and Ag ions. Interestingly, in the comparative toxicity test in which the AgNPs concentration was fixed at 5 mg/L and Ag ions were increased, the toxicity was lower than when bacteria were exposed to AgNPs and Ag ions independently (Fig. 4c). However, bioavailable Ag ions released from AgNPs promoted a higher and different toxicity to E. coli K-12 strain during the tests when the Ag concentration was fixed and the AgNPs concentration was increased, compared to when the toxicity to AgNPs and Ag ions was tested independently (Fig. 4d). Therefore, it became evident that AgNPs and Ag ions have unique relationships that affect their toxicity to E. coli K-12 strain under diverse coexistence conditions, and this must be considered a different toxicity parameter than purely a sum of their independent effects.

We subsequently investigated the toxicity of AgNPs and Ag ions to E. coli K-12 strain in conjunction with L-cysteine under different exposure conditions (Fig. 5). When AgNPs and Ag ions were combined with L-cysteine, the bioavailable Ag ions released from AgNPs were reduced. The thiol (–SH) group binding sites of

L-cysteine can associate with Ag ions, and have been shown to begin connecting immediately on contact (Kim et al., 2008; Levard et al., 2012). Therefore, L-cysteine can effectively bind Ag ions, not only when Ag ions exist alone, but also when AgNPs and Ag ions coexist. When *E. coli* K-12 strain is simultaneously treated with AgNPs and Ag ions, they grow more actively with L-cysteine than without it. Moreover, L-cysteine can help the cells to initially adapt and thereby accelerate the growth rate. Therefore, L-cysteine bound the Ag ions when AgNPs and Ag ions coexisted and reduced their toxicity to *E. coli* K-12 strain.

4. Conclusions

Overall, this investigation provides a useful understanding of the toxicity of AgNPs and how they compare with the toxicity of Ag ions to *E. coli* K-12 strain, both when the AgNPs and Ag ions occur independently and when they coexist. Different conditions of coexistence of AgNPs and Ag ions displayed the decreased toxicity to *E. coli* K-12 strain, even when Ag ions were added. This toxicity condition represents a tendency different from that from AgNPs and Ag ions when existing independently. Therefore, AgNPs and Ag ions were seen to have a different toxicity relationship when they coexist and may thus be subject to a new chemical process affecting the release of Ag ions from AgNPs. Here, the release of bioavailable Ag ions from AgNPs promoted a higher toxicity, with the addition of L-cysteine then reducing the bioavailable Ag ions released from the AgNPs. A future work needs to evaluate and monitor the toxicity of AgNPs to various other organisms and to consider additional environmental factors such as pH, ionic strength, and natural organic matter (NOM). Finally, this study also may represent a new horizon for producing of NPs having less toxicity and greater stability in the environment by using environmental friendly synthesis methods.

Acknowledgments

Appendix A. Supplementary data

Supplementary data to this article can be found online at http://dx.doi.org/10.1016/j.jes.2017.04.028.

REFERENCES

Apel, K., Hirt, H., 2004. Reactive oxygen species: metabolism, oxidative stress, and signal transduction. Annu. Rev. Plant Biol. 55, 373–399.

Aquilano, K., Baldelli, S., Ciriolo, M.R., 2014. Glutathione: new roles in redox signaling for an old antioxidant. Front. Pharmacol. 5, 196.

Blaser, S.A., Scheringer, M., Macleod, M., Hungerbuhler, K., 2008. Estimation of cumulative aquatic exposure and risk due to silver: contribution of nano-functionalized plastics and textiles. Sci. Total Environ. 390 (2–3), 396–409.

Buffet, P.E., Pan, J.F., Poirier, L., Amiard-Triquet, C., Amiard, J.C., Gaudin, P., et al., 2013. Biochemical and behavioural responses of the endobenthic bivalve *Scrobicularia plana* to silver nanoparticles in seawater and microalgal food. Ecotoxicol. Environ. Saf. 89, 117–124.

Dasgupta, N., Ramalingam, C., 2016. Silver nanoparticle antimicrobial activity explained by membrane rupture and reactive oxygen generation. Environ. Chem. Lett. 14 (4), 477–485.

Frohlich, E., 2012. The role of surface charge in cellular uptake and cytotoxicity of medical nanoparticles. Int. J. Nanomedicine 7, 5577–5591.

Gaiser, B.K., Fernandes, T.F., Jepson, M.A., Lead, J.R., Tyler, C.R., Baalousha, M., et al., 2012. Interspecies comparisons on the uptake and toxicity of silver and cerium dioxide nanoparticles. Environ. Toxicol. Chem. 31 (1), 144–154.

Gao, J., Powers, K., Wang, Y., Zhou, H., Roberts, S.M., Moudgil, B.M., et al., 2012. Influence of Suwannee River humic acid on particle properties and toxicity of silver nanoparticles. Chemosphere 89 (1), 96–101.

Handy, R.D., Owen, R., Valsami-Jones, E., 2008. The ecotoxicology of nanoparticles and nanomaterials: current status, knowledge gaps, challenges, and future needs. Ecotoxicology 17 (5), 315–325.

He, D., Dorantes-Aranda, J.J., Waite, T.D., 2012. Silver nanoparticle–algae interactions: oxidative dissolution, reactive oxygen species generation and synergistic toxic effects. Environ. Sci. Technol. 46, 8731–8738.

Hsin, Y.H., Chen, C.F., Huang, S., Shih, T.S., Lai, P.S., Chueh, P.J., et al., 2008. The apoptotic effect of nanosilver is mediated by a ROS- and JNK-dependent mechanism involving the mitochondrial pathway in NIH3T3 cells. Toxicol. Lett. 179 (3), 130–139.

Katz, L.M., Dewan, K., Bronaugh, R.L., 2015. Nanotechnology in cosmetics. Food Chem. Toxicol. 85, 127–137.

Kim, J.Y., Lee, C., Cho, M., Yoon, J., 2008. Enhanced inactivation of *E. coli* and MS-2 phage by silver ions combined with UV-A and visible light irradiation. Water Res. 42 (1–2), 356–362.

Kim, H.A., Choi, Y.J., Kim, K.W., Lee, B.T., Ranville, J.F., 2012. Nanoparticles in the environment: stability and toxicity. Rev. Environ. Health 27 (4), 175–179.

Kim, I., Lee, B.-T., Kim, H.-A., Kim, K.-W., Kim, S.D., Hwang, Y.-S., 2016. Citrate coated silver nanoparticles change heavy metal toxicities and bioaccumulation of *Daphnia magna*. Chemosphere 143, 99–105.

Levard, C., Hotze, E.M., Lowry, G.V., Brown, G.E., 2012. Environmental transformations of silver nanoparticles: impact on stability and toxicity. Environ. Sci. Technol. 46 (13), 6900–6914.

Li, X., Schirmer, K., Bernard, L., Sigg, L., Pillai, S., Behra, R., 2015. Silver nanoparticle toxicity and association with the alga *Euglena gracilis*. Environ. Sci.: Nano 2 (6), 594–602.

Lu, H., Fan, W., Dong, H., Liu, L., 2017. Dependence of the irradiation conditions and crystalline phases of TiO_2 nanoparticles on their toxicity to *Daphnia magna*. Environ. Sci.: Nano.

Lubick, N., 2008. Nanosilver toxicity: ions, nanoparticles—or both? Environ. Sci. Technol. 42 (23), 8617-8617.

Marambio-Jones, C., Hoek, E.M.V., 2010. A review of the antibacterial effects of silver nanomaterials and potential implications for human health and the environment. J. Nanopart. Res. 12 (5), 1531–1551.

Matzke, M., Jurkschat, K., Backhaus, T., 2014. Toxicity of differently sized and coated silver nanoparticles to the bacterium *Pseudomonas putida*: risks for the aquatic environment? Ecotoxicology 23 (5), 818–829.

Maurer, L.L., Meyer, J.N., 2016. A systematic review of evidence for silver nanoparticle-induced mitochondrial toxicity. Environ. Sci.: Nano 3 (2), 311–322.

McGillicuddy, E., Murray, I., Kavanagh, S., Morrison, L., Fogarty, A., Cormican, M., et al., 2017. Silver nanoparticles in the environment: sources, detection and ecotoxicology. Sci. Total Environ. 575, 231–246.

Navarro, E., Baun, A., Behra, R., Hartmann, N.B., Filser, J., Miao, A.-J., et al., 2008a. Environmental behavior and ecotoxicity of engineered nanoparticles to algae, plants, and fungi. Ecotoxicology 17 (5), 372–386.

Navarro, E., Piccapietra, F., Wagner, B., Marconi, F., Kaegi, R., Odzak, N., et al., 2008b. Toxicity of silver nanoparticles to *Chlamydomonas reinhardtii*. Environ. Sci. Technol. 42 (23), 8959–8964.

Nel, A., Xia, T., Madler, L., Li, N., 2006. Toxic potential of materials at the nanolevel. Science 311 (5761), 622–627.

Nowack, B., Bucheli, T.D., 2007. Occurrence, behavior and effects of nanoparticles in the environment. Environ. Pollut. 150 (1), 5–22.

Nowack, B., Ranville, J.F., Diamond, S., Gallego-Urrea, J.A., Metcalfe, C., Rose, J., et al., 2012. Potential scenarios for nanomaterial release and subsequent alteration in the environment. Environ. Toxicol. Chem. 31 (1), 50–59.

Park, H.J., Kim, J.Y., Kim, J., Lee, J.H., Hahn, J.S., Gu, M.B., et al., 2009. Silver-ion-mediated reactive oxygen species generation affecting bactericidal activity. Water Res. 43 (4), 1027–1032.

Peng, Y.H., Tsai, Y.C., Hsiung, C.E., Lin, Y.H., Shih, Y.H., 2017. Influence of water chemistry on the environmental behaviors of commercial ZnO nanoparticles in various water and wastewater samples. J. Hazard. Mater. 322 (Pt B), 348–356.

Pham-Huy, L.A., He, H., Pham-Huy, C., 2008. Free radicals, antioxidants in disease and health. Int. J. Biomed. Sci. 4 (2), 89–96.

Rahal, A., Kumar, A., Singh, V., Yadav, B., Tiwari, R., Chakraborty, S., et al., 2014. Oxidative stress, prooxidants, and antioxidants: the interplay. Biomed. Res. Int. 2014, 761264.

Ratte, H.T., 1999. Bioaccumulation and toxicity of silver compounds: a review. Environ. Toxicol. Chem. 18 (1), 89–108.

Ren, C., Hu, X., Zhou, Q., 2016. Influence of environmental factors on nanotoxicity and knowledge gaps thereof. NanoImpact 2, 82–92.

Robbens, J., Dardenne, F., Devriese, L., Coen, W.D., Blust, R., 2010. *Escherichia coli* as a bioreporter in ecotoxicology. Appl. Microbiol. Biotechnol. 88, 1007–1025.

Silver, S., Phung, L.T., Silver, G., 2006. Silver as biocides in burn and wound dressing and bacterial resistance to silver compounds. J. Ind. Microbiol. Biotechnol. 69 (7), 4278–4281.

Sondi, I., Salopek-Sondi, B., 2004. Silver nanoparticles as antimicrobial agent: a case study on E. *coli* as a model for Gram-negative bacteria. J. Colloid Interface Sci. 275 (1), 177–182.

Steven, L., Fiedler, A.V., 2010. Simulation of nanoparticles permeation through a lipid membrane. Biophys. J. 99, 144–152.

Wang, Y., Li, C., Yao, C., Ding, L., Lei, Z., Wu, M., 2016a. Techniques for investigating molecular toxicology of nanomaterials. J. Biomed. Nanotechnol. 12 (6), 1115–1135.

Wang, Z., Zhang, L., Zhao, J., Xing, B., 2016b. Environmental processes and toxicity of metallic nanoparticles in aquatic systems as affected by natural organic matter. Environ. Sci.: Nano 3 (2), 240–255.

Wei, L., Lu, J., Xu, H., Patel, A., Chen, Z.S., Chen, G.F., 2015. Silver nanoparticles: synthesis, properties, and therapeutic applications. Drug Discov. Today 20 (5), 595–601.

Weiss, L., Zeigel, R., 1971. Cell surface negativity and the binding of positively charged particles. J. Cell. Physiol. 77 (2), 179–185.

Wu, Y., Zhou, Q., 2013. Silver nanoparticles cause oxidative damage and histological changes in medaka (*Oryzias latipes*) after 14 days of exposure. Environ. Toxicol. Chem. 32 (1), 165–173.

Wu, F., Harper, B.J., Harper, S.L., 2017. Differential dissolution and toxicity of surface functionalized silver nanoparticles in small-scale microcosms: impacts of community complexity. Environ. Sci.: Nano.

Xu, P., Xu, J., Liu, S., Yang, Z., 2012. Nano copper induced apoptosis in podocytes via increasing oxidative stress. J. Hazard. Mater. 241-242, 279–286.

Yin, L., Cheng, Y., Espinasse, B., Colman, B.P., Auffan, M., Wiesner, M., et al., 2011. More than the ions: the effects of silver nanoparticles on *Lolium multiflorum*. Environ. Sci. Technol. 45 (6), 2360–2367.

Zhang, F., Wu, X., Chen, Y., Lin, H., 2009. Application of silver nanoparticles to cotton fabric as an antibacterial textile finish. Fibers Polym. 10 (4), 496–501.

Zhang, Z., Yang, X., Shen, M., Yin, Y., Liu, J., 2015. Sunlight-driven reduction of silver ion to silver nanoparticle by organic matter mitigates the acute toxicity of silver to *Daphnia magna*. J. Environ. Sci. 35, 62–68.